

Thermal effects and dynamical hysteresis in the turn-on and turn-off of vertical-cavity surface-emitting lasers

Yanhua Hong,^{1,*} Cristina Masoller,² Maria S. Torre,³ Sanjay Priyadarshi,¹
Abdulqader A. Qader,¹ Paul S. Spencer,¹ and K. Alan Shore¹

¹Bangor University, School of Electronic Engineering, Dean Street, Bangor, LL57 1UT, Wales, UK

²Departament de Física i Enginyeria Nuclear, Universitat Politècnica de Catalunya, Colom 11, E-08222 Terrassa, Spain

³Instituto de Física, Universidad Nacional del Centro de la Provincia de Buenos Aires, Pinto 399 (7000), Tandil, Argentina

*Corresponding author: y.hong@bangor.ac.uk

Received May 11, 2010; revised June 16, 2010; accepted October 4, 2010;
posted October 11, 2010 (Doc. ID 128304); published October 28, 2010

Thermal effects and dynamical hysteresis in VCSELs under dc modulation have been experimentally studied. The results show that the VCSEL turn-on and turn-off currents can display both positive hysteresis and negative hysteresis, depending on the current modulation frequency and on the substrate temperature. Numerical simulations of semiconductor laser rate equations, extended to take into account thermal effects, show a good agreement with the observations. © 2010 Optical Society of America

OCIS codes: 140.5960, 250.7260.

Directly modulated, long-wavelength VCSELs are attractive components for the fast-growing market of high-speed optical communication systems [1]. VCSELs have many advantages compared with edge-emitting lasers, such as low cost, compact size, low threshold current, circular output-beam profile, and wafer-scale integrability, but in contrast to 850 nm VCSELs, long-wavelength VCSELs have a relatively large spectral detuning between the gain and the cavity resonance at room temperature [2]. This results in increased temperature sensitivity, which can have an impact on the performance of directly modulated devices [3].

A recent numerical study [4] has shown thermally induced hysteresis on the laser switch-on and switch-off points, which depends on the relationship between two time scales: that of the current modulation, which results in dynamical hysteresis [5,6], and that of thermal dissipation, which is an additional source of hysteresis that can give either positive or negative [7,8] hysteresis cycles. In positive cycles, the laser turns on at a higher current value than it turns off; in negative cycles, the turn-on occurs at a lower current value than the turn-off. Temperature-induced hysteresis depends on the current modulation frequency: if the modulation is too fast, thermal effects do not have time to act; and if the current modulation is too slow, the dynamics are quasi-static and thermal equilibrium is reached before the bias current changes appreciably.

The aim of this Letter is to study experimentally and theoretically the influence of the current modulation frequency and the substrate temperature on the VCSEL threshold current and gain a better understanding of thermal effects in VCSELs. The experimental results show that the hysteresis of turn-on and turn-off can be positive or negative, depending on the current modulation frequency and substrate temperature, in good agreement with the numerical results [4]. Numerical simulations that are in good qualitative agreement with the experiments are also presented and allow for a better understanding

of the interplay of the time scales of current modulation and thermal dissipation.

In the experiment, a VCSEL with lasing wavelength of about 1550 nm was used. It operates on a single longitudinal and transverse mode and exhibits no polarization switching within the current operating range. The VCSEL was driven by an ultra-low-noise current source and was temperature controlled to within 0.01 °C. A triangular direct modulation signal was added to the VCSEL through the current source. The dc bias current was set at 4 mA and the modulation amplitude was 3.7 mA, so the bias current was scanned from 0.3 to 7.7 mA. The output of the VCSEL was collimated by an antireflection-coated laser diode objective lens. The orthogonal polarization components of the VCSEL were divided by a half-wave plate and a polarization beam splitter. Two optical isolators with more than -40 dB isolation were used to prevent feedback into the VCSEL. The output of the orthogonal polarizations was recorded simultaneously by 1 GHz bandwidth detectors and stored in a 4 GHz bandwidth digital oscilloscope.

Figure 1 displays the light-current ($L-I$) curve when the current modulation frequency is 10 kHz and the substrate temperature is 10 °C [Fig. 1(a)] and 60 °C [Fig. 1(b)]. In spite of the fact that VCSELs often display polarization switching when the pump current varies, the device employed in these experiments operates in a single stable linear polarization within the experimental operating range; therefore, only the output of that lasing polarization is plotted. The black curve is for increasing current and the gray curve (red online) is for decreasing current. The insets display in detail the threshold current. It can be seen that the threshold with increasing current, termed the turn-on threshold, I_{on} , does not overlap the threshold with decreasing current, termed the turn-off threshold, I_{off} . There is hysteresis between I_{on} and I_{off} : in the case of low substrate temperature, $I_{\text{on}} > I_{\text{off}}$ (this type of hysteresis is termed positive hysteresis); in the case of high substrate temperature, $I_{\text{on}} < I_{\text{off}}$ (this type of hysteresis is termed negative hysteresis).

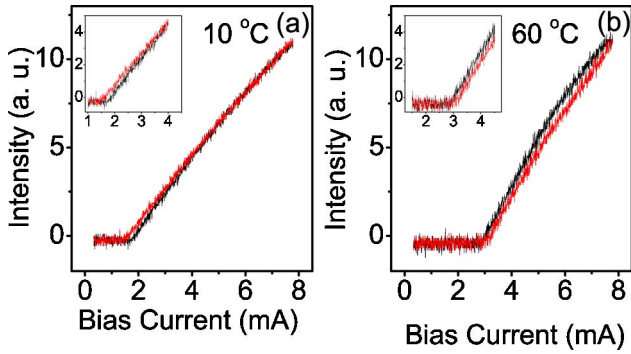


Fig. 1. (Color online) L-I curve of the VCSEL with 10 kHz modulation frequency for (a) 10 °C and for (b) 60 °C substrate temperature. The black curve is for increasing current; the gray curve (red online) is for decreasing current. The insets display details of the threshold currents.

Figure 2 shows the turn-on and turn-off currents as a function of the substrate temperature for various modulation frequencies. It can be noticed that both I_{on} and I_{off} increase with the substrate temperature, but the rates of variation are different—except for the slow 1 Hz modulation frequency, in which these are equal within the operation range of substrate temperatures and correspond to the static threshold current. A parabolic-like dependence of the static threshold with the substrate temperature can be observed, in good agreement with previous experimental and theoretical studies [9,10]. When the modulation frequency increases to 1 kHz, as shown in Fig. 2(b), I_{on} and I_{off} show hysteresis at substrate temperatures higher than 30 °C. It is apparent that $I_{\text{on}} < I_{\text{off}}$; thus, there is a negative hysteresis cycle. When the modulation frequency is between 5 and 20 kHz, as shown in Figs. 2(c)–2(e), $I_{\text{on}} > I_{\text{off}}$ (positive hysteresis) at low substrate temperature and $I_{\text{on}} < I_{\text{off}}$ (negative hysteresis) at high substrate temperature. With further increase of the modulation frequency to 100 kHz, I_{on} and I_{off} show only positive hysteresis, $I_{\text{on}} > I_{\text{off}}$.

Figure 3 shows the size of the hysteresis cycle as a function of the modulation frequency for different substrate temperature. It is seen that the curves have similar trends for all substrate temperatures. For lower modulation frequencies, there is no clear hysteresis between the turn-on and turn-off currents. When the modulation

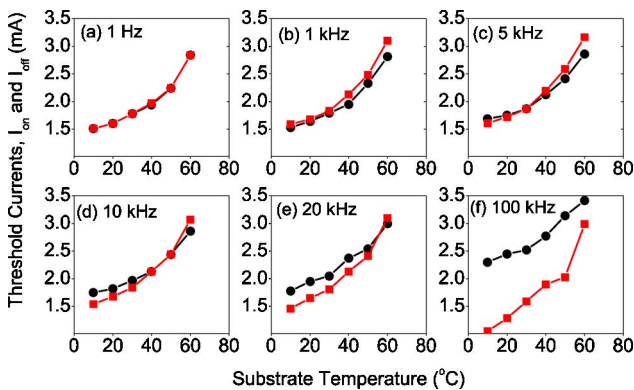


Fig. 2. (Color online) Threshold currents as a function of the substrate temperature for various modulation frequencies. The black circles and the gray squares (red online) indicate I_{on} and I_{off} , respectively.

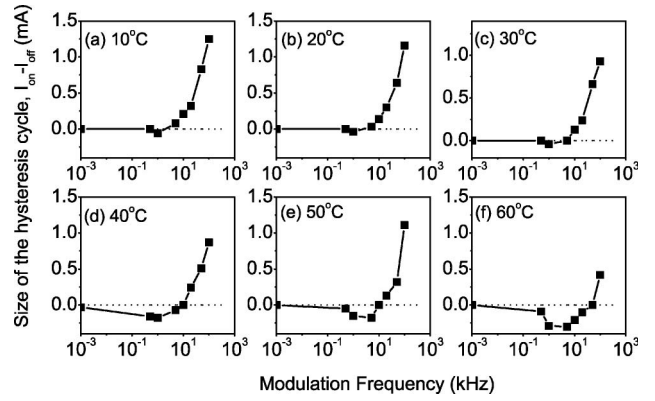


Fig. 3. Size of the hysteresis cycle, $I_{\text{on}} - I_{\text{off}}$ as a function of the modulation frequency at various values of the substrate temperatures.

frequency is increased over a certain value, $I_{\text{on}} - I_{\text{off}}$ decreases and becomes negative. With further increase of the modulation frequency, $I_{\text{on}} - I_{\text{off}}$ grows and becomes positive at high frequency.

The hysteresis of I_{on} and I_{off} can be explained as due to the interplay of current modulation and thermal effects. Current modulation results in dynamical hysteresis [5,6], and the temperature variation is an additional source of hysteresis. For 50 °C and 60 °C substrate temperature, when the modulation frequencies are 1 and 5 kHz, these combined effects result in negative hysteresis. As will be further discussed below, this occurs due to the fact that, because of the heating of the device, both the gain peak wavelength, λ_g , and the cavity mode wavelength, λ_c , redshift, but their redshift rates are different. Thus, I_{on} can either decrease or increase with respect to the static threshold, depending on the relation between the thermal dissipation rate, the current modulation frequency, and the rates of variation of λ_g and λ_c . When the modulation frequencies are increased up to 100 kHz, then slowly responding thermal effects do not have time to act and only positive dynamical hysteresis is observed.

The rate equations for a semiconductor laser, incorporating the dynamic variation of the temperature of the active region are [4,10]

$$\dot{E} = \frac{1}{2}k(1 + j\alpha)(gN - 1)E + \sqrt{\beta_{\text{sp}}\gamma_N}\xi, \quad (1)$$

$$\dot{N} = \gamma_N(\mu - N - gN|E|^2), \quad (2)$$

$$\dot{T} = -\gamma_T(T - T_s) + Z\left(\frac{N}{K} + 1\right) + P\left(\frac{\mu}{K} + 1\right)^2, \quad (3)$$

where E is the complex slowly varying optical field, N is the normalized carrier density, and T is the active region temperature. Other parameters are linewidth enhancement factor α , the coefficient of spontaneous emissions β_{sp} , the field decay rate k , the carried decay rate γ_N , and the normalized injection current $\mu = K(I/I_0 - 1)$, where I is the bias current, I_0 is the current needed to reach transparency, and K is a dimensionless constant. In the temperature equation, γ_T takes into account the

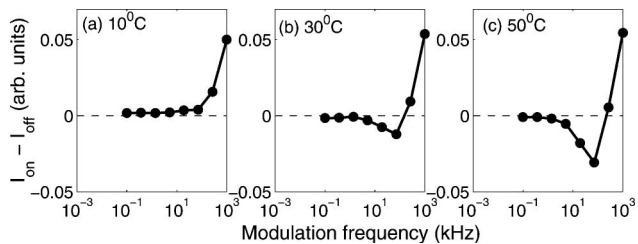


Fig. 4. Numerically calculated size of the hysteresis cycle, $I_{\text{on}} - I_{\text{off}}$, versus the modulation frequency at three values of the substrate temperatures.

decay rate to the substrate temperature, T_s , and Z and P represent nonradiation recombination heating and Joule heating, respectively. The gain coefficient, g , is a Lorentzian in the frequency space, $g(\omega, T) = g_0(T) / \{1 + [\delta(T) - \omega]^2 / \Delta\omega_g^2(T)\}$, where $\delta(T) = \omega_g(T) - \omega_c(T)$ is the gain-cavity offset, $\omega = \text{Im}(\dot{E}/E)$ is the slowly varying optical frequency, $g_0 = T_0/T$ is the gain peak, and $\Delta\omega_g^2 = \Delta\omega_{g,0}^2(T/T_0)$ is the gain bandwidth, with T_0 being the reference room temperature [4,10].

The model equations were integrated with typical parameters appropriate for a 1550 nm VCSEL: the room temperature gain-cavity offset, $\delta_0 = -10$ nm, $\gamma_N = 1$ ns⁻¹, $\gamma_T = 1$ μ s⁻¹, $Z = 8.5 \times 10^{-3}$, $P = 9.2 \times 10^{-5}$, and all other parameters as in [4,10]. The size of the hysteresis cycle versus the modulation frequency at three values of the substrate temperature is displayed in Fig. 4, and one can notice that there is a qualitatively good agreement with the experimental observations.

In conclusion, thermal effects and dynamical hysteresis in the turn-on and turn-off of directly modulated VCSELs were studied experimentally and numerically. The hysteresis can be explained in terms of the interplay of dynamical hysteresis (due to current variation), thermal dissipation, and device heating, which is an additional source of hysteresis because of the redshift of both gain peak and the cavity resonance with increasing temperature. At high substrate temperature, the interplay of these effects can give negative hysteresis in a certain range of modulation frequencies; at low frequencies, the dynamics are quasi-static and there is no hysteresis, and at high frequencies, slow thermal effects do not have time to act and there is only normal dynamical hysteresis.

Our results are relevant, as they provide a complete picture of the various time scales on which heating effects come into play and affect the device performance. A good understanding of thermal effects is important not

only for low-frequency modulation of VCSELs but also at high frequencies, where the first-order response function has a cutoff frequency [11] that cannot be explained by models that only take into account the laser fast time scales (the photon and carrier lifetimes). We have compared the observations with the results of a rate-equation model that, in spite of using a simple expression for the optical gain and neglecting spatial effects (carrier and temperature diffusion), allows for a good understanding of thermal effects in a straightforward way, with a great reduction of computational time as compared with detailed microscopic models.

The authors thank RayCan Ltd and Prof. K. H. Kim, Inha University, South Korea, for the supply of VCSELs. S. P. is supported by Bangor University. C. M. and M. S. T. are supported in part by the U.S. Air Force Office of Scientific Research (USAFOSR) under grant FA8655-10-1-3075. C. M. also acknowledges the ICREA foundation for financial support and the Spanish Ministerio de Educacion y Ciencia through projects FIS2008-06024-C03-02 and FIS2009-13360.

References

1. X. Zhao, B. Zhang, L. Christen, D. Parekh, W. Hofmann, M. C. Amann, F. Koyama, A. E. Willner, and C. J. Chang-Hasnain, *Opt. Express* **17**, 13785 (2009).
2. S. Mogg, N. Chitica, U. Christiansson, R. Schatz, P. Sundgren, C. Asplund, and M. Hammar, *IEEE J. Quantum Electron.* **40**, 453 (2004).
3. Y. Hong, J. Paul, P. S. Paul, and K. A. Shore, *IEEE J. Quantum Electron.* **44**, 30 (2008).
4. M. S. Torre and C. Masoller, "Dynamical hysteresis and thermal effects in vertical-cavity surface-emitting lasers," *IEEE J. Quantum Electron.* (to be published).
5. J. R. Tredicce, G. L. Lippi, P. Mandel, B. Charasse, A. Chevalier, and B. Picqué, *Am. J. Phys.* **72**, 799 (2004).
6. J. Paul, C. Masoller, Y. Hong, P. S. Paul, and K. A. Shore, *Opt. Lett.* **31**, 748 (2006).
7. D. Bromley, E. J. D'Angelo, H. Grassi, C. Mathis, and J. R. Tredicce, *Opt. Commun.* **99**, 65 (1993).
8. S. Sivaprakasam, D. N. Rao, and R. S. Pandher, *Opt. Commun.* **176**, 191 (2000).
9. C. Chen, P. O. Leisher, A. A. Allerman, K. M. Geib, and K. D. Choquette, *IEEE J. Quantum Electron.* **42**, 1078 (2006).
10. C. Masoller and M. S. Torre, *Opt. Express* **16**, 21282 (2008).
11. G. Verschaffelt, J. Albert, B. Nagler, M. Peeters, J. Danckaert, S. Barbay, G. Giacomelli, and F. Marin, *IEEE J. Quantum Electron.* **39**, 1177 (2003).